The long-term genetic stability and individual specificity of the human gut microbiome

The long-term genetic stability and individual specificity of the human gut microbiome

Lianmin Chen [1,2,*], Daoming Wang [1,*], Sanzhima Garmaeva [1], Alexander Kurilshikov [1], Arnau Vich Vila [1,3], Ranko Gacesa [1,3], Trishla Sinha [1], LifeLines Cohort Study, Eran Segal [4,5], Rinse K. Weersma [3], Cisca Wijmenga [1], Alexandra Zhernakova [1,#] and Jingyuan Fu [1,2,6,#]

[1] Department of Genetics, University Medical Center Groningen, University of Groningen, Groningen, the Netherlands

[2] Department of Pediatrics, University Medical Center Groningen, University of Groningen, Groningen, the Netherlands

[3] Department of Gastroenterology and Hepatology, University Medical Center Groningen, University of Groningen, Groningen, the Netherlands

[4] Department of Computer Science and Applied Mathematics, Weizmann Institute of Science, Rehovot, Israel

[5] Department of Molecular Cell Biology, Weizmann Institute of Science, Rehovot, Israel

[6] Lead Contact

*These authors contributed equally

#Correspondence: j.fu@umcg.nl and sashazhernakova@gmail.com

HIGHLIGHTS (max 85 characters)

- Gut microbial composition with higher baseline diversity is more stable over time
- Gut microbial genetic makeup is more personal specific than composition
- Individual-specific and temporally stable microbial profiles fingerprint the host
- Plasma metabolites can mediate microbial impact on host health

SUMMARY (max 150)

By following up the gut microbiome, 51 human phenotypes and plasma levels of 1,183 metabolites in 338 individuals after four years, we characterize the microbial stability and variation in relation to host's physiology. We made use of individual-specific and temporally stable microbial profiles, including bacterial SNPs and structural variations, to built a microbial fingerprinting model, which shows 82% accuracy in classifying metagenomic samples four year apart. Application of our model in independent cohort (HMP) provide 95% accuracy for classification of samples one year apart. Simultaneously, we observed temporal changes in the abundance of multiple bacterial species, metabolic pathways and structural variation, as well as strain replacement. We report 258 longitudial microbial associations with the host's phenotype and 519 associations with plasma metabolites. The association was enriched for cardiometabolic traits, vitamin B and uremic toxins. Mediation analysis pintpoints many metabolites that mediate the microbial impact on the host, providing evidence as therapeutic targets.

Keywords: gut microbiome, stability, taxonomy, pathway, SNP, copy number variation, genomic deleation, metabolites, strain replacement, fingerprint

INTRODUCTION

Human guts harbor a diverse community of microbes that exhibit large between-individual variations (Falony et al., 2016; Lloyd-Price et al., 2017; Rothschild et al., 2018; Zhernakova et al., 2016), and cross-sectional analyses have now linked these variations to human health and disease phenotypes (Chen et al., 2020a; Falony et al., 2016; Rothschild et al., 2018; Vieira-Silva et al., 2020; Zhernakova et al., 2016). The gut microbiota also undergoes compositional changes over the course of an individual's life, either as the cause or consequence of changes in host health and disease status (Chen et al., 2018; Vatanen et al., 2018; Zhou et al., 2019). Several studies have assessed temporal changes in microbial taxonomical composition (Faith et al., 2013; Mehta et al., 2018) and laid the foundation for targeted mechanistic investigations of the consequences of host–microbiome crosstalk for health and disease, including studies in early childhood (Stewart et al., 2018), early-onset type 1 and type 2 diabetes (Vatanen et al., 2018; Zhou et al., 2019) and inflammatory bowel disease (Lloyd-Price et al., 2019).

Nevertheless, several important questions about the temporal variability of the gut microbiome remain unexplored. Firstly, beyond gut microbial composition, the genetic makeup of microbial genomes can also undergo dynamic changes over time. Microbial genomic changes due to evolution and strain replacement, such as single nucleotide mutations and gain or loss of genomic regions (structural variation), implicate putative mechanism for the development of human disease (Greenblum et al., 2015; Schloissnig et al., 2013; Zeevi et al., 2019). Yet investigations of temporal changes in microbial genetic makeup are still missing. Secondly, while cross-sectional association analyses have reported numerous associations with host health and disease (Falony et al., 2016; Lloyd-Price et al., 2017; Rothschild et al., 2018; Zhernakova et al., 2016), these associations lack longitudinal confirmation that would allow us to assess whether alterations of the gut microbiome are related to changes in host health status. Thirdly, other microbial components such as antibiotic resistance and virulence factors have

become a major concern given the wide-scale use of antibiotics in the last decades. The risk of transfer of resistance and virulence genes between microorganisms has been extensively investigated due to its relevance to human health (Ochman et al., 2000). However, information on the spread of antibiotic resistance and virulence genes among human gut commensal microorganisms over time has not yet been reported, which impedes the effective prevention and treatment of bacterial infections.

In this study, we present a long-term follow-up analysis of the gut microbiome in 338 participants of the population-based Lifelines-DEEP cohort (Tigchelaar et al., 2015), in which we compared samples taken four years apart. We characterized long-term temporal stability in the gut microbial composition and genetic makeup and aimed to answer two types of questions: 1) Which bacterial features not only show individual specificity but also temporal stable? Can we use such features as the fingerprint to distinguish samples from the same individual. 2) Which bacterial features show large temporal variation? Can their temporal variation be linked to the changes of host's clinical phenotypes and lifestyles. To further gain biological insights, we profiled plasma levels of 1183 metabolites at both time points and aimed to construct in-silico causal inference of microbial impact on host's health through metabolites using mediation analysis. Finally, we assessed the increase of antibiotic resistance and virulence factors in the human gut microbiome, which may indicate the urgency of fighting infectious disease.

RESULTS

The LifeLines-DEEP follow-up cohort

To investigate the long-term variability of the human gut microbiome, we collected fecal samples from 338 individuals from the prospective, population-based Lifelines-DEEP cohort taken four years apart (Tigchelaar et al., 2015) and processed these samples using the same lab protocols and bioinformatic pipelines. 51 phenotypic factors were assessed at both time points, including intrinsic factors (e.g. age, sex and body mass index), blood cell counts, plasma metabolites (e.g. glucose, HbA1c and blood lipid profile), diseases and medication usage **(Table S1)**. We observe significant temporal changes for 19 phenotypic factors four years apart at FDR<0.05 (**Figure S1, Table S1**). For instance, significant increases were observed for plasma levels of creatinine ($P_{Paired\ Wilcoxon}=2.5x10^{-50}$), systolic blood pressure ($P_{Paired\ Wilcoxon}=3.6x10^{-26}$), and blood basophil granulocytes cell counts ($P_{Paired\ Wilcoxon}=8.2x10^{-39}$) (**Figure S1, Table S1**). We also observed changes in lifestyle, diseases and medication usage (**Table S1**). For example, compared to the baseline, the number of smokers was reduced by 4.5%, and 17 participants started using proton pump inhibitors (PPI), while 6 stopped.

Temporal changes in the gut microbial diversity and compostion

To characterize the stability of the gut microbiome over time, we first investigated microbial composition and diversity. Compared to baseline, we observed a significant increase in the alpha-diversity (Shannon index based on species, $P_{Paired\ Wilcoxon}=2.4x10^{-7}$, **Figure 1A**), as well as a moderate variation in microbial taxonomical and functional composition ($P_{PCo1\ Paired\ Wilcoxon}>0.082$ and $P_{PCo2\ Paired\ Wilcoxon}<1.6x10^{-5}$ for both species and pathway, **Figure S2**). The differences in overall microbial taxonomical and functional composition were larger between individuals than within-individuals ($P_{Wilcoxon}<1x10^{-4}$, **Figure 1B&C**), indicating that even after four years an individual's gut microbial composition is more similar to itself than to those of other people. Interestingly, within-individual differences in gut microbial composition were smaller in participants with a higher alpha-diversity at baseline ($r_{Spearman}=-0.21$, $P=1.5x10^{-4}$,

Figure 1D), supporting the hypothesis that a diverse microbial communities tend to be more stable (Coyte et al., 2015).

When comparing individual microbial species and pathways, the relative abundance of 59.9% species (94 out of 157) and 44.3% pathways (152 out of 343) showed significant changes at FDR<0.05 (paired Wilcoxon test, **Table S2a&b**). Species belonging to the same genera often showed consistent changes in direction, e.g. the relative abundance of seven *Bifidobacterium* species all decreased significantly, while the abundances of the majority of *Alistipes* species (7 out of 8) increased (**Table S2a**). These changes may partially be due to the age effect. For instance, several *Bifidobacterium* species including *B. adolescentis*, *B. bifidum* and *B. longum* have been observed to be negatively associated with age (Zhernakova et al., 2016).

Microbial genetic stability differs substantially across species

Microbial genetic makeup may also change over time, e.g. due to mutagenesis and strain replacement as a consequence of selective pressure. Characterization of the stable and changeable genetic components of the gut microbiome over a long time-course is important for further understanding the importance of microbial strains alterations with respect to host phenotypic changes. Here, we characterized within-individual temporal microbial genetic changes by comparing both single nucleotide polymorphism (SNP) haplotypes (Truong et al., 2017) and genomic structural variants (SVs) (Zeevi et al., 2019). SNP haplotype differences were characterized for 37 species that were present in at least 5 paired samples from both time points (**Figure 2A, Table S2c**). We also identified 6,130 SVs, including 4,333 deletion SVs (absence of genomic regions) and 1,797 variable SVs (genomic regions with variable copy numbers) from 41 microbial species in at least 5 paired samples (**Figure 2B, Table S2d**). For 23 species, both strain SNP haplotype and SV information were available (**Figure 2A&B**).

We observed that within-individual genetic changes in terms of both SNP haplotypes and SVs were significantly smaller than the differences observed between different

individuals (**Figure 2A&B**, **Table S2c&d**). The species that showed large temporal changes in their SNP haplotypes include *Ruminococcus torques*, *Streptococcus parasanguinis* and *Faecalibacterium prausnitzii,* while *Bifidobacterium angulatum*, *Methanobrevibacter smithii* and *Alistipes putredinis* showed relatively low genetic variability ($P_{Wilcoxon}$<0.05, **Figure 2A**). A consistent trend in genetic stabilities in terms of SNP profile was observed in 43 healthy participants with fecal microbiome data abailable one year apart from the Human Microbiome Project (HMP) (**Figure 2C**) (Schloissnig et al., 2013). Compared to the HMP cohort, the genetic difference of unstable species were larger in the LLD cohort potentially due to a longer time duration (**Figure 2D-F**). This observation further supports the genetic instability of these species over time.

Temporal variability in SNP haplotypes and SVs also showed consistency (**Figure S3**), suggesting that the microbial genetic stability of some species can be seen at different genetic variation levels. For example, several species with highly variable SNP haplotypes over time, such as *R. torques* and *F. prausnitzii*, also showed a high degree of changes in their SVs, while some species, such as *M. smithii*, showed high stability of both SNP haplotypes and within-individual SVs variability (**Figure 2A&B**).

Interestingly, these genetic unstable species have often been reported to be related to human health and disease. For instance, previous studies have shown a higher abundance of *R. torques* in patients with Crohn's disease (Joossens et al., 2011), a higher level of *S. parasanguinis* in patients with intestinal infection (Vacca, 2017), and a lower level of *F. prausnitzii* in paitents with inflammatory bowel disease (Munukka et al., 2017; Vich Vila et al., 2018). Notably, within-individual changes in microbial genetic makeup did not correlate with changes in abundance (**Figure S4**), suggesting that microbial genetic variability provides a new layer of information that is independent of microbial abundance. Furthermore, the observed temporal changes in genetic make-up can be also due to strain replacement. For instance, we could detect distinct strains based on SNP profiles in *R. torques*, *F. prausnitzii*, *S. parasanguinis*, *Ruminococcus*

obeum and *Eubacterium rectale* (**Figure S5**). For instance, we observed two distinct strain clusters in *F. prausnitzii* (**Figure 3A, Figure S5**) and found that strain replacement happened in 37 participants (**Figure 3B**).

Taken together, these results illustrate that within-individual variations in both microbial composition and genomes can be seen four years apart, but within-individual similarity of microbiome compositional and genetic profiles is greater than between-individual similarity. The observed stable and variable microbial compositional and genetic components can have different implications: the individually stable microbial components might be used to identify their host, while the variable microbial components might reveal their clinical relevance in relation to phenotypic changes.

Microbial genetic makeups show individuality that serve as host fingerprint

We observed that some species, such as *M. smithii,* showed large between-individual variability but small within-individual variability in their genetic makeup (**Figure 2A**). Per 100 base pairs (bp) of the species-specific regions, *M. smithii* had an on average 0.11 bp difference between two samples from the same individual but an average 2.78 bp difference between different individuals ($P_{Wilcoxon\ test}=3.6x10^{-64}$, **Figure 2A**, **Table S2c**). This led us to evaluate the possibility of using microbial genetic and compositional profiles to identify samples from the same individuals. We could generate the SNP haplotype profiles of *M. smithii* for 100 paired samples. Based on the distance of the *M. smithii* SNP profiles, we could correctly link 94 paired individuals, resulting in an accuracy of 94% (**Figure S6A**). Another example was the SNP profile of *Phascolarctobacterium succinatutens* that can classify 41 paired samples with 88% of accuracy (**Figure S6B**). Notably, sample classification based on microbial composition and pathway profile could only result in 12% and 5% accuracy, respectively (**Table S3**). Our data prove that microbial genetic profiles can be applied as an individual fingerprint and that genetic profiles of the gut microbiome greatly outperform species and pathway abundance profiles in individual identification.

Due to low abundance and insufficient read coverage in some samples, SNP haplotype profiles like *M. smithii* could only be generated for 100 out of 338 paired samples, which prohibits the use of the genetic profile of one single species as a host fingerprint. This limitation inspired us to combine multiple microbial genetic and composition (both species and pathway abundances) distance matrices for a broader application. We applied stepwise forward selection to optimize the combination of different numbers of distance matrices in 60% of randomly selected individuals and validated the individual recognition abilities in the remaining 40% of individuals. The resampling and feature selection were repeated 10 times (**Figure S7**). The combination of all 71 distance matrices (**Table S3**) resulted in up to 85% classification accuracy (**Figure 4A**), and an optimal model combining the top 30 distance matrices yielded 82% classification accuracy (**Figure 4B**). This optimal model includes SNP profiles of 13 species, deletion SV profiles of 11 species, variable SV profiles of 5 species and the Bray-Curtis dissimilarity of species abundance (**Figure S8**). We also conducted the specificity and sensitivity analyses in sample classification. The total area under curve (AUC) was 95% (**Figure 3C**) and we reached the optimal 99% of specificity and 88% of sensitivity at the distance cutoff 0.46 (**Figure 3D**). At this cutoff, we obstained 298 paired samples with 93% of accurancy.

We further applied our microbial fingerpint model in the longitudial sample collection of 43 individuals in the HMP cohort. Our model resulted in 100% of accuracy for 41 out of 43 paired samples at the distance cutoff 0.46 (**Figure 3B**) and 95% of accuracy in the total set of 43 pairs. The accuracy is much higher than the previously reported 30% accuracy based on microbial abundance only (Franzosa et al., 2015). This result has confirmed the robustness of our microbial fingerprint method, suggesting its broad application in longitudinal microbiome studies.

Microbial abundance and genomic changes associated with host phenotypes

To examine the role of the gut microbiota in host health, we explored the associations

between microbial compositional and genomic changes and host phenotypic changes. We performed two-step analyses to reveal microbial associations to host phenotypes using longitudinal data. First, we performed joint association analyses between microbial features and 27 host phenotypic factors that were highly prevalent between the two time points (**Table S1**) by using mixed models and including age, sex and sampling time as covariates. Next, for associations identified at FDR<0.05, we conducted regression analysis on temporal differences, i.e. associations between microbial changes and host phenotypic changes over time (delta association). The identified 258 associations (involving 225 microbial features and 39 phenotypes) that were significant at FDR<0.05 in the joint association analysis and also significant at P<0.05 for the delta association analysis with a consistent direction of effect. These included 113 associations with species and pathway abundances and 145 associations with microbial SVs (**Figure 5A**, **Table S4a**).

In line with the significant changes in blood pressure and other cardiometabolic phenotypes four years apart, we detected multiple associations to the temporal changes of the gut microbiome (**Table S4a**). The top associations included a positive association between systolic blood pressure and the abundance *Lachnospiraceae bacterium* ($beta_{delta}$= 0.24, P_{delta}= $1.1x10^{-5}$, **Figure 5B**) and a negative association between glycated hemoglobin (HbA1c) and flavin biosynthesis pathway ($beta_{delta}$= -0.22, P_{delta}= $4.9x10^{-5}$, **Figure 5C**). We also observed that the prevence of heart rhythm problems associated with the absence of a genomic region (927-928kb) in *Collinsella sp* that encodes the branched-chain amino acids transport system ($P_{Fisher\ exact\ test}$= $5.0x10^{-4}$, **Figure 5E**). Besides, we observed association of temporal changes in microbial SVs with host immune phenotypes. For instance, a variable SV (3019-3020kb) in *Blautia obeum* that contains virulence protein E and chloramphenicol resistance genes negatively associated with the change of blood lymphocyte cell counts ($beta_{delta}$= -0.29, P_{delta}= $6.5x10^{-4}$, **Figure 5D**).

Microbial abundance and genomic changes associated with plasma metabolites

To further understand the potential mechanisms by which the gut microbiota could drive host pathophysiology, we hypothesized that metabolites are an important class of molecultes that is involved in host-microbe interaction. By profiling plasma levels of 1,183 metabolites in both timepoints with untargeted LC-MS, we observed that 27% of metabolites showed significant difference between two timepoints at FDR<0.05 (Paired Wilcoxon, **Table S2e**).

We first checked whether plasma metabolites showed difference in participants with distnict microbial strains of five genetical unstable species (**Figure S5**), and if so, whether strain replacements of these species were related to changes in plasma metabolites. In total, 64 associations were observed between 63 metabolites and strain clusters of five species (**Table S4b**). For example, we identified two distinct strain clusters of *F. prausnitzii* in 292 paired samples (**Figure 3A**), which associated with 15 metabolites. The top associations were observed for licorisoflavan A, pyrrole and p-cresol sulfate, which abundances were significantly lower in the individuals with *F. prausnitzii* strain cluster2. Consistenly, we observed that the abundance of these metabolites decreased in 24 individuals where *F. prausnitzii* swifted from strain cluster1 to cluster2, while their metabolite levels increased in 13 inviduals where *F. prausnitzii* swifted from strain cluster2 to cluster1(**Figure 3C-E**). This result implicates that different microbial strains may have different functions that influence host metabolism.

Apart from it, temporal changes in microbial abundance and SVs may also relevant for host metabolic changes. In total, 455 significant associations were detected between 122 microbial features (species and pathway abundances, dSVs and vSVs) and 81 metabolites (FDR_{joint}<0.05 and P_{delta}<0.05, **Figure 6A**, **Table S4c**), including 273 associations with microbial abundance and 182 associations with microbial SVs. Interestingly, various metabolites that associated with microbiome are known to be related to the gut microbiome. For instance, we detected 38 microbial associations to plasma thiamine levels, a vitamin (B1) produced by gut microbes and its deficiency affecting the cardiovascular system and inducing a fast heart rate (DiNicolantonio et al.,

2013). The top microbial associations to thiamine include species *Alistipes senegalensis* ($beta_{delta}$= 0.20, P_{delta}= 4.1x10^{-4}, **Figure 6B**), *Bacteroidales bacterium* ($beta_{delta}$= 0.23, P_{delta}= 5.2x10^{-5}), and TCA cycle pathway ($beta_{delta}$= 0.23, P_{delta}= 7.2x10^{-5}) (**Table S4c**). Notably, genome of *Alistipes senegalensis* contains genes responsible for thiamine biosynthesis (Mishra et al., 2012).

Another interesting category of metabolites are protein-bound uremic toxins, which are related to microbial metabolism of amino acids and have been associated with various chronic diseases (Wang and Zhao, 2018). We have characterized plasma levels of 58 uremic toxins from metabolite categories of indoxyl sulfate, p-cresyl sulfate, phenyl sulfate, phenylacetic acid and hippuric acid (Wang and Zhao, 2018), and observed a significant enrichment for microbial associations, i.e., a total of 97 associations for 16 uremic toxins (Fisher's exact test P=1.7x10^{-21}) (**Figure 6A**, **Table S4c**). The most associated uremic toxins included p-cresol (24 associations), p-cresol sulfate (20 associaitons) and hippuric acid (16 associations) (**Table S4c**). p-cresol sulfate is a microbiota-drived metabolite that contributes to many biological and biochmemical effects, such as albuminuria in diabetic kidney disease (Kikuchi et al., 2019). The top association to p-cresol sulfate was *Bacteroidales bacterium ph8* ($beta_{delta}$= 0.21, P_{delta}= 1.9x10^{-4}, **Figure 6C**), a gut microbial species with limited information available yet. Notably, 22.6% of (103 out of 455) microbial asosciations with metabolites were related to vSVs of *Blautia wexlerae* (**Figure 6A**). Among them, 27 associations were related to different uremic toxins, particularly to hippuric acid (**Figure 6D**), an acyl glycine formed from the conjugation of benzoic acid with glycine and associated with phenylketonuria, propionic acidemia and tyrosinemia (Duranton et al., 2012). Intriguingly, these vSV regions that encode various membranes transporters, amino acid kinases, urease accessory protein and protein bingding genes (**Table S5**).

Microbiome contributed to host phenotypic changes through its metabolites

For 225 microbial features associated with clinical phenotypes and 122 associations to metabolites, 29 microbial features were associated with both clinical phenotypes and

metabolites (**Figure 7A**). We explored whether these metabolites can mediate the microbial impact on host's phenotypes. By using bi-directional mediation analysis, 21 mediation relationships were established ($FDR_{mediation}$<0.05 and $P_{inverse\ mediation}$>0.05, **Figure 7B**, **Table S4d**). The identified mediation effects were mostly related to microbial impact on blood pressure via thiamine and acetyl-N-formyl-5-methoxykynurenamine (AFMK). The impact of thiamine on cardiometabolic health has been well documented and a randomized controlled trial has showed that thiamine can reduce diastolic blood pressure (Alaei-Shahmiri et al., 2015). AFMK is the degradation metabolite of melatonin, which contributes to blood pressure reduction by inhibiting the synthesis of prostaglandin (Mayo et al., 2005; Rezzani et al., 2010). Our mediation analysis suggested that various bacterial pathways may contribute to these effects. For instance, microbial sulfate reduction pathway can lower diastolic blood pressure through increasing the plasma level of thiamine levels (21%, $P_{mediation}= 6.0x10^{-3}$, **Figure 7C**) and bacterial lipopolysaccharides biosynthesis may lead to a decrease of systolic blood pressure through affecting plasma level of AFMK (16%, $P_{mediation}= 6.0x10^{-3}$, **Figure 7D**). Metabolic products like cysteine from bacterial sulfate reduction pathway is essential for bacterial thiamine (vitamin B1) biosynthesis (Begley, 1996), and lipopolysaccharides can activate melatonin oxidized into AFMK (Silva et al., 2004).

We also identified several mediation effects of metabolites on microbial impact on plasma lipids and glucose levels (**Figure 7B**). An interesting one is tyrosol 4-sulfate, an uremtic toxin that mediates the effect of a vSV in *Ruminococcus sp* (300 to 305 kb) on plasma levels of LDL (17%, $P_{mediation}= 0.017$, **Figure 7E**). This vSV contains an ATPase that responsible for metabolites transmembrane transport (Aguilar-Barajas et al., 2011).

Significant increase of microbial antibiotic resistance

The increase of antibiotic resistance can pose a great burden in fighting infectious diseases, while the virulence factors are essential for the commensal microbiota to maintain colonization niche and evade the host's immune response. We further systematically characterized and compared the abundances of 29 antibiotic resistance

genes and 59 virulence genes over time. We observed a significant increase in the total antibiotic resistance gene load ($P=1.1x10^{-9}$) and a decrease in the total number of virulence genes ($P=5.1x10^{-4}$) (**Figure 8A&B**). At the individual gene level, 55.17% (16 out of 29) of antibiotic resistance genes and 18.64% (11 out of 59) of virulence genes showed a significant difference (FDR<0.05) between time points (**Table S2f&g**). Specifically, 15 out of 16 antibiotic resistance genes showed an increase in their abundance, with the highest change observed for tetracycline resistance genes (**Figure S9**), such as tetracycline resistance protein Q (TetQ) that is widely distributed in *Bacteroides* species (Veloo et al., 2019). In line with this, the increase of tetracycline resistance gene abundance was associated with the increased abundance of multiple *Bacteroides* species (e.g. *B. vulgatus*, *B. uniformis* and *B. ovatus*, **Figure 8C**, **Table S4e**) whose abundance also increased in the follow-up (**Table S2a**).

Through antibiotic prescription in the Netherlands remains the lowest in the Europe, tetracycline, aminoglycoside and lincosamide are among the top broad spectrum veterinary antibiotics (Havelaar et al., 2017), which may contribute to the increased microbial antibiotic resistance in humans (Aslam et al., 2018). We thus examined the correlation of baseline meat intake with the abundance changes of microbial antibiotic resistance genes and found positive associations with aminoglycoside ($r_{Spearman}= 0.18$, $P= 9.2x10^{-4}$) and lincosamide resistance ($r_{Spearman}= 0.15$, $P= 5.5x10^{-3}$) (**Figure 8D&E**, **Table S4f**). These observations raise concerns about antibiotic usage in farming, which may contribute to the spread of microbial antibiotic resistance in the human gut ecosystem.

DISCUSSION

Over the past years, numerous associations between a disrupted microbiota and diseases, for example gastrointestinal and cardiometabolic diseases, have been observed in large cross-sectional studies (Chen et al., 2020a; Chen et al., 2020b; Falony et al., 2016; Rothschild et al., 2018; Vieira-Silva et al., 2020; Zhernakova et al., 2016). However, the key to understanding the role of a disrupted microbiota in human diseases is to

366 answer how stable the microbiota is and whether within-individual microbial changes
367 can be linked to changes in host health status. We therefore systematically characterized
368 the microbial changes at both compositional and genomic level at two time points four
369 years apart in 338 individuals from the Lifelines-DEEP cohort. We observed that the
370 gut microbiome to some extent showed long-term within-individual stability in both
371 microbial abundance and microbial genome. Particularly, we found that the genetic
372 makeup of microbes shows individuality that can be used as a fingerprint to distinguish
373 metagenomic samples belonging to the same individual. In addition, the longtitudial
374 association analysis between the changes of gut microbiome, host phenotypic, as well
375 as human plasma metabolites have provided in-sillico causal relationships and putative
376 mechanistic insights regarding the importance of the gut microbiome on human health.
377 Finally, we observed that increased microbial antibiotic resistance in the human gut
378 microbiome was associated with meat consumption.

379 Previous investigations on short-term (within one year) temporal stability of microbial
380 composition and genetic makeup in adults revealed that metagenomic samples obtained
381 from the same individual are more similar to one another than to those from different
382 individuals (Garud et al., 2019; Mehta et al., 2018). Large-scale characterization of the
383 long-term (four years apart) stability of the gut microbiome in a present study extended
384 this observation. In addition, we found that within-individual differences in gut
385 microbial composition were smaller in participants who had a higher alpha-diversity at
386 baseline, supporting the hypothesis that the microbial communities with higher
387 diversity tend to be more stable over time (Coyte et al., 2015).

388 We also observed that genetic stability of gut microbes vary substantially across
389 differenct species, and a set of species from, but not limited to genus *Bacteroides*,
390 *Bifidobacterium*, *Methanobrevibacter* and *Phascolarctobacterium* showed relatively
391 high within-individual stability over a long period of time. Notably, previous study
392 showed that some of these species, such as *Bacteroides* and *Bifidobacterium* species
393 are colonized at early life (Yassour et al., 2018) and showed high genetic stability in

childhood (Vatanen et al., 2019). These data suggests that each person is likely to have individual-specific microbial genetic components that are distinct from those of others, and may span from childhoold to adulthood. The gut microbial genetic profile can therefore serve as a host fingerprint to uniquely distinguish stool samples that belong to the same host. In this study, we constructued a novel microbial finger printing model that combines 30 microbial features, including microbial composition, SNP profiles of 13 species and structural variation of 16 species. Our model has the accuracy of sample identification to 82% in the Lifelines-DEEP samples that were taken four years apart. By applying our model to the HMP samples up to one year apart, our model resulted in 95% of accurarcy, significantly outperforming the previous method based on microbial composition only, which resulted in only 30% accuracy (Franzosa et al., 2015). These results demonstrate the potential application of our method in distinguishing sample mix up, but also raise potential privacy concerns for subjects enrolled in human microbiome research projects.

Characterization of the long-term changes of the gut microbiome is crucial for understanding the role of the gut microbiome in chronic disease, the diseases being of long duration and generally slow progression. Differential microbial abundances have been characterized for around half of microbial species and pathways, and within-individual changes in microbial genetic makeup have also been observed. Interestingly, the bacterial SNP haplotype and SV changes did not associate with abundance changes, which reveals a potential new layer of information about the microbiome's contribution to host health that is independent of abundance alterations. Our study reported a total of 258 associations between microbial changes with phenotypic changes over time. Moreover, by assessing the plasma level of 1,183 metabolites at both time points, we reported 519 associations between microbial changes with metabolic changes, including 273 associations with abundance of species and metabolic pathways, 64 associations with strain replacement, and 182 associations with alternation in structural variation. In contrast to previous studies that only focused on microbial abundance

associations to host phenotypes (Lloyd-Price et al., 2019; Vatanen et al., 2018; Zhou et al., 2019), the microbial genetic associations that connect genomic variation with genetically encoded function to phenotypic changes can provide putative mechanistic information. We noticed that genetically unstable species (e.g. *R. torques*, *S. parasanguinis* and *F. prausnitzii*) have been associated with various human diseases (Joossens et al., 2011; Ray et al., 2014; Vacca, 2017; Zhernakova et al., 2016). *F. prausnitizii* can support mucasal immune homeostatsis (Hornef and Pabst, 2016), which has been mostly linked to its capacity of butyrate production (Miquel et al., 2013). However, our data shows that the higher increase in a variable SV of *F. prausnitzii* was associated with the lower increase in the number of lymphocytes cells. This SV region encodes multiple toxin degradation genes. Interestingly, we also observed *F. prausnitizii* strain replacement in 37 individuals and established many associations with plasma metabolites, including Licorisolfavan A and p-cresal sulfate from the class of isofavonoids and uremic toxins that affect host's immunity. Thereby our data together suggests novel mechansims underlying the role of *F. prausnitzii* in host's immunity.

Notably, metabolite associations to the gut microbiome were significantly enriched for uremic toxins and thiamine (vitamin B1). Uremic toxins are derived by gut microbiota from dietary protein and the accumulation of uremic toxins can induce chronic sterile inflammation, which in turn increases the risk of kidney and cardiometabolic diseases (Solomon et al., 2010). We characterized 58 protein-binding uremic toxins and detected 97 associations for 16 uremic toxins. One of the mostly associated uremic toxins is hippuric acid, a cardiometabolic risk related metabolite that can significantly contribute to the prediction of weight gaining (Yu et al., 2018; Zhao et al., 2016). We observed several novel microbial associations with hippuric acid, such as the associations between *B. wexlerae* SVs and hippuric acid. These *B. wexlerae* SVs were also associated with BMI, implicating *B. wexlerae* may contribute to metabolic disorder potentially through hippuric acid metabolism.

Vitamin B1 production is dependent on the gut microbiome, and the deficiency can

infulence the cardiovascular system (DiNicolantonio et al., 2013). Among microbial associations to vitamin B1, the top association was related to *Akkermansia muciniphila* abundance, a well-known benefical microbe that controls gut barrier function and homeostatic functions (Everard et al., 2013). Our mediation analysis identified 21 relationships that the metabolites can mediate the microbial impact on host phenotype, particularly for cardiometabolic traits. With this analysis, we further revealed that *A. muciniphila* may infulance blood pressure through vitamin B1 production, a rationale for the development of a treatment that uses this human mucus colonizer for the prevention of hypertension. All together, our longitudinal microbial association and mediation analyses on host phenotypes and plasma metabolites provided novel functional insights and putative causality regarding the role of the gut microbiome in human health and disease.

Furthermore, our study provide evidence that antibiotics used in animal husbandry can result in the increase of the antibiotic resistance genes in the human gut microbome. Regulating and promoting the appropriate use of veterinary antibiotics should be considered by public health policy makers.

Limitations of Study

We acknowledge several limitations in our study. Our study sampled fecal samples four year apart in 338 samples. To date, it is the longtidual microbiome study with the longest duration and largest sample size. We systematically investigated the compositional and genetic variation over time and link the microbial changes to phenotypic changes. However, our sample size was still limited. Many of our findings need further replication in independent cohorts with longer duration and larger sample size. For example, we observed that gut microbial composition with higher baseline diversity is more stable over time. The observed effect was modest and needs to be further validated. Moreover, the Lifelines-DEEP cohort is comprised of participants from northern area of the Netherlands and with only Dutch ethnicity. It is possible that the reported results are biased towards a region-specific microbial background due to

host's genetics and local environmental exposures. Despite the possible bias, the performance of our novel microbial finger printing model has been successfully validated in the HMP cohort. Furthermore, the reported longitudinal association are not a proof of causation even though we applied casual mediation analysis to refer in-sillico causality. We primarily focused on biologically plausible mechanisms by intergrating longitudinal metabolism dataset and provides mechanistic hypotheses that pinpoint to specific microbial genetics and function but also demonstrate which metabolites are likely to mediate the impact of the gut microbiome on the host's phenotype. Experimental validation is warranted.

ACKNOWLEDGEMENTS

We thank the participants and staff of the LifeLines-DEEP cohort for their collaboration. We thank J. Dekens and J. Arends for management and technical support and K. Mc Intyre for English editing. This project was funded by the Netherlands Heart Foundation (IN-CONTROL CVON grant 2012-03 and 2018-27 to A.Z. and J.F.); the NWO Gravitation Netherlands Organ-on-Chip Initiative to J.F. and C.W., the NWO Gravitation Exposome-NL (024.004.017) to J.F., A.K., and A.Z.; the Netherlands Organization for Scientific Research (NWO) (NWO-VIDI 864.13.013 to J.F., NWO-VIDI 016.178.056 to A.Z., NWO-VIDI 016.136.308 to R.K.W. and NWO Spinoza Prize SPI 92-266 to C.W.); the European Research Council (ERC) (FP7/2007-2013/ERC Advanced Grant 2012-322698 to C.W. and ERC Starting Grant 715772 to A.Z.); the RuG Investment Agenda Grant Personalized Health to C.W.; and the Foundation De Cock-Hadders grant (20:20-13) to L.C. L.C. also holds a joint fellowship from the University Medical Centre Groningen and China Scholarship Council (CSC201708320268). D.W. holds a fellowship from the China Scholarship Council (CSC201904910478). S.G. holds a fellowship from the Graduate School of Medical Sciences, University of Groningen. R.K.W. is supported by the Seerave Foundation and the Dutch Digestive Foundation (16-14). The funders had no role in the study design, data collection and analysis, decision to publish, or preparation of the

manuscript.

AUTHOR CONTRIBUTIONS

C.W., A.Z. and J.F. conceptualized and managed the study. L.C., W.D., S.G., A.K., A.V.V., R.G. and T.S. generated the data. L.C., W.D., S.G. and A.K. analyzed the data. L.C., D.W., S.G. and J.F. drafted the manuscript. L.C., W.D., S.G., A.K., A.V.V., R.G., T.S., E.S., R.K.W., C.W., A.Z. and J.F. reviewed and edited the manuscript.

COMPETING INTERESTS

The authors declare no competing interests.

FIGURE LEGENDS

Figure 1. Long-term stability of the gut microbiome composition. A. The gut microbial alpha diversity (Shannon index) increased after four years. **B** & **C.** Within-individual changes in microbial species and pathway composition were lower than between-individual differences. **D.** Temporal changes in microbial composition (species-level Bray-Curtis dissimilarity) were negatively associated with baseline alpha diversity.

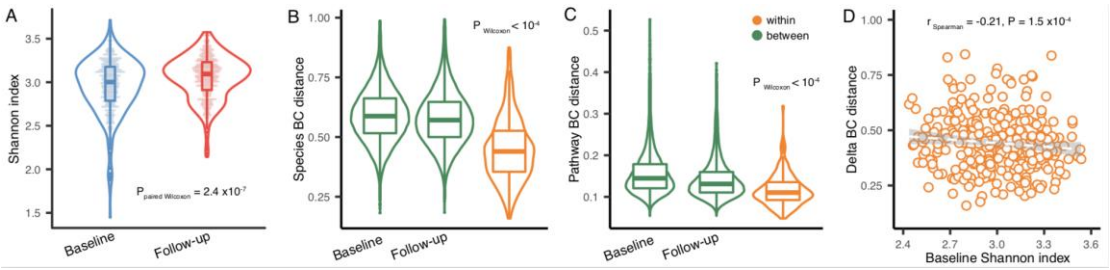

Figure 2. Long-term stability of microbial species SNP haplotypes and structural variants. A. Within- and between-individual differences in the single nucleotide polymorphism (SNP) haplotypes of dominant strains of microbial species. Numbers follow species names incidate the number of paired samples for which SNP haplotype profiles are available four years apart. **B.** Within- and between-individual difference in the deletion and variable structural variants (SVs) of microbial strains. Numbers follow species names incidate the number of paired samples for which SVs profiles are available four years apart. **C.** Comparison of within-individual microbial species SNP haplotype difference between the LLD (four years apart) and the HMP (one year apart). Each dot represents one species. Dots marked in orange represent SNP haplotype differences show difference between the LLD and the HMP at FDR< 0.05 (Wilcoxon test). **D, E & F.** Within-individual SNP haplotype differences in genetical unstable *Ruminococcus torques*, *Faecalibacterium prausnitzii* and *Eubacterium rectale* show difference between the LLD and the HMP.

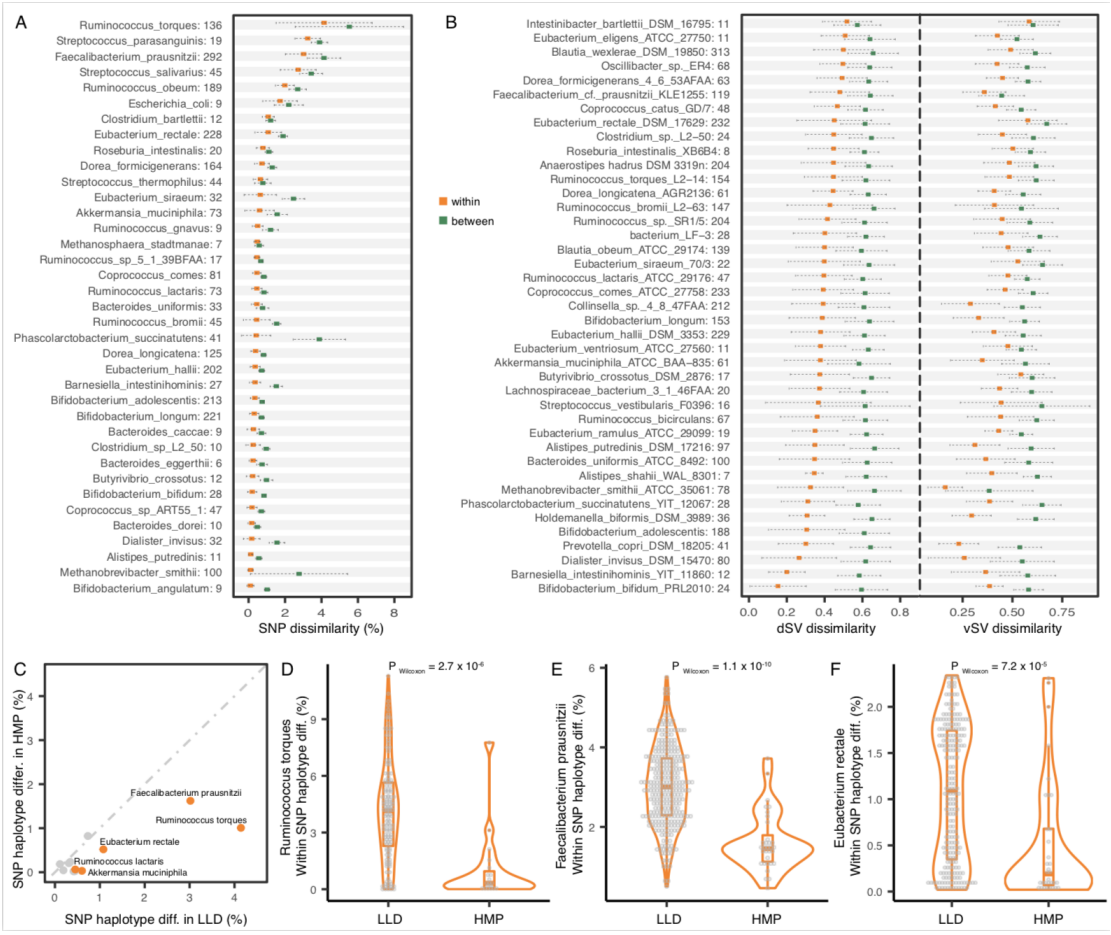

536

537 **Figure 3. *Faecalibacterium prausnitzii* strain replacement associated with plasma**
538 **metabolite changes. A.** Two disnict *F. prausnitzii* strain clusters based on its SNP
539 haplotype profile. **B.** Within-individual *F. prausnitzii* strain switches four years apart.
540 **C, D & E.** Plasma levels of licorisoflavan A, 1,2,5-Trimethyl-1H-pyrrole and p-cresol
541 sulfate showed difference between disnict *F. prausnitzii* strains, and *F. prausnitzii* strain
542 switches associated with changes of these metabolites.

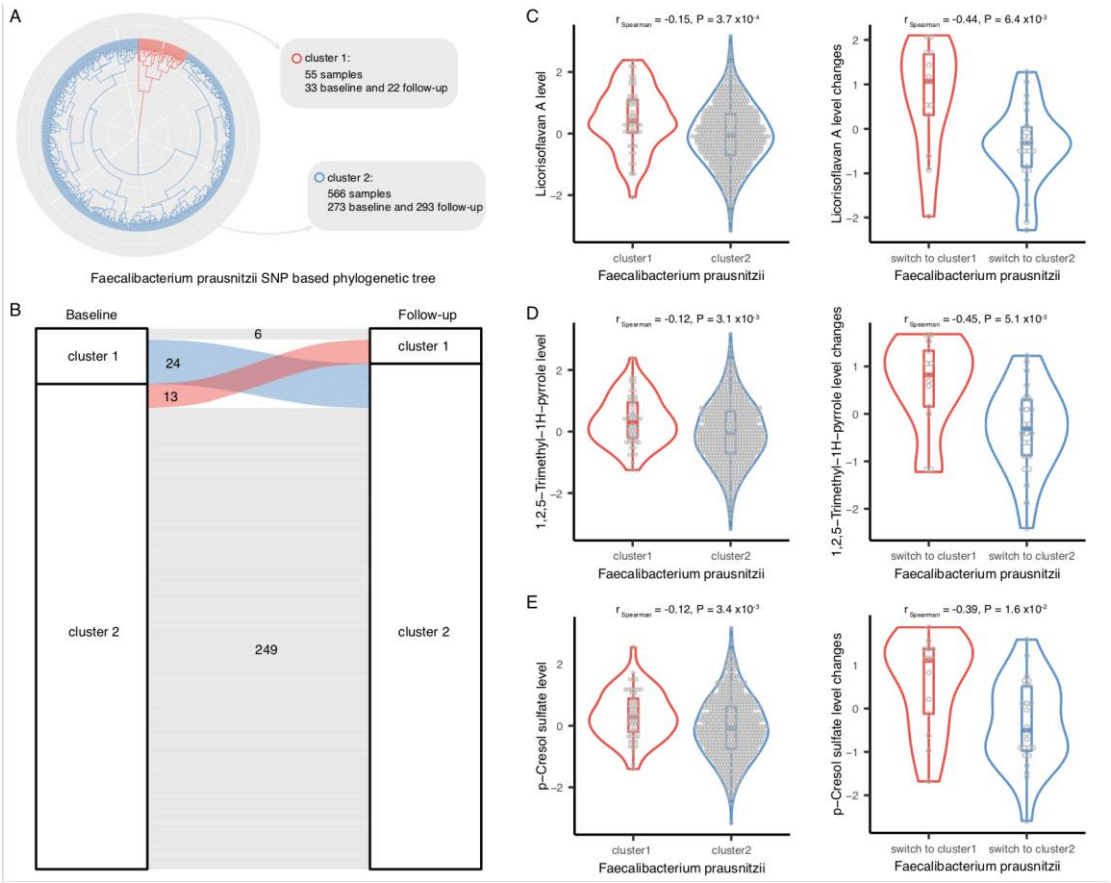

Figure 4. Performance of the gut microbiome in fingerprinting its human host. A. The combination of all microbial genetic and compositional profiles resulted in up to 85% accuracy in distinguishing 676 metagenomic samples from 338 individuals four years apart. A combination of 30 microbial genetic and compositional profiles resulted in an accuracy of 82% in the LLD. **B.** The combination of 30 microbial genetic and compositional profiles resulted in an accuracy of 95% in the HMP cohort that involved 43 participants with metagenomics abailable one year apart. **C.** A combination of 30 microbial genetic and compositional profiles resulted in 95% and 99% AUCs for the LLD and the HMP individual classification in ROC analysis, respectively. **D.** The distribution of within- and between-individual distances in the combined distance matrices. At a cutoff of 0.46, the classification performance in terms of both specificity and sensitivity reached optimally.

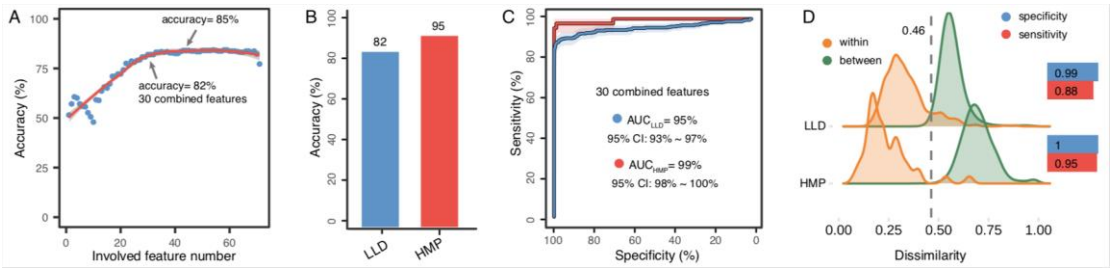

Figure 5. Association of microbial temporal changes with host phenotypic changes. **A.** Summary of microbial associations to phenotypes. A total of 258 associations were not only significant at FDR<0.05 for the joint association analysis, but also significant at P<0.05 for the association analysis of temporal changes, with the same effect direction of both analyses. These include 113 associations to species and pathway abundances and 145 associations to microbial SVs. **B.** Positive association between systolic blood pressure and *Lachnospiraceae bacterium* abundance changes. **C.** Negative association between plasma HbA1c and fungi flavin biosynthesis pathway abundance changes. **D.** Increased *Blautia obeum* vSV (3019-3020 kb) variabilities associated with the decreased blood lymphocyte counts. **E.** Presence rate of *Collinsella sp 4_8_47FAA* dSV (927-928 kb) showed difference between the presence and absence of heart rhythm problems.

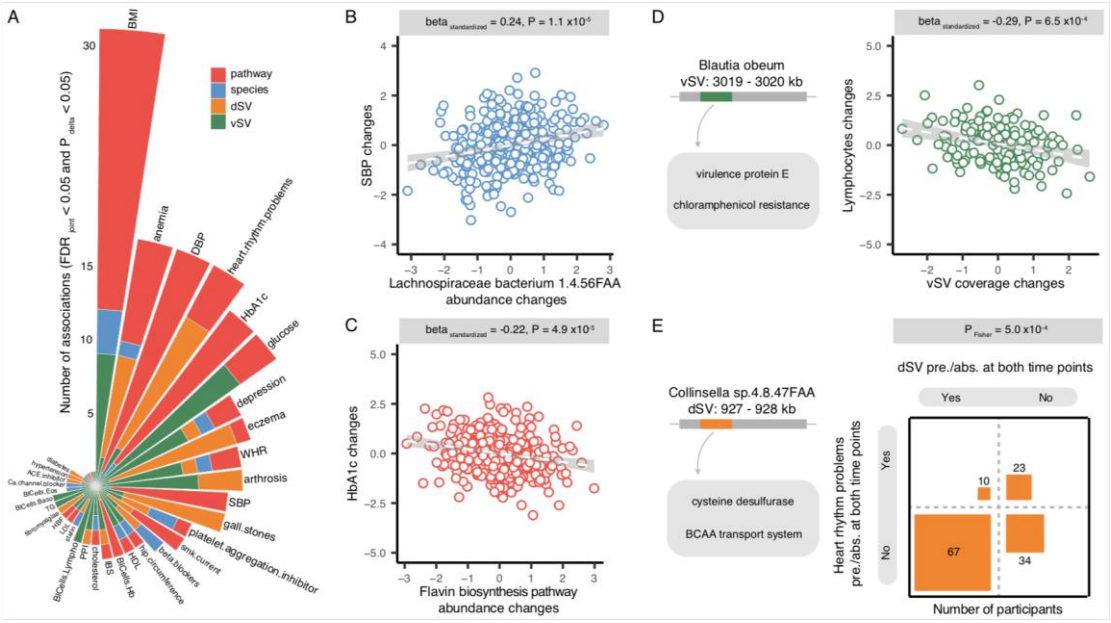

Figure 6. Association of microbial temporal changes with plasma metabolite changes. A. Summary of microbial associations to plasma metabolites. A total of 455 associations were not only significant at FDR<0.05 for the joint association analysis, but also significant at P<0.05 for the association analysis of temporal changes, with the same effect direction of both analyses. These include 273 associations to species and pathway abundances and 182 associations to microbial SVs. **B.** A positive association between thiamine and *Alistipes senegalensis* abundance changes. **C.** The positive association between microbial-derived uremic toxin p-cresol sulfate and *Bacteroidales bacterium* abundance changes. **D.** Variability changes in multiple vSVs of *Blautia wexlerae* associated with microbial drived uremic toxins.

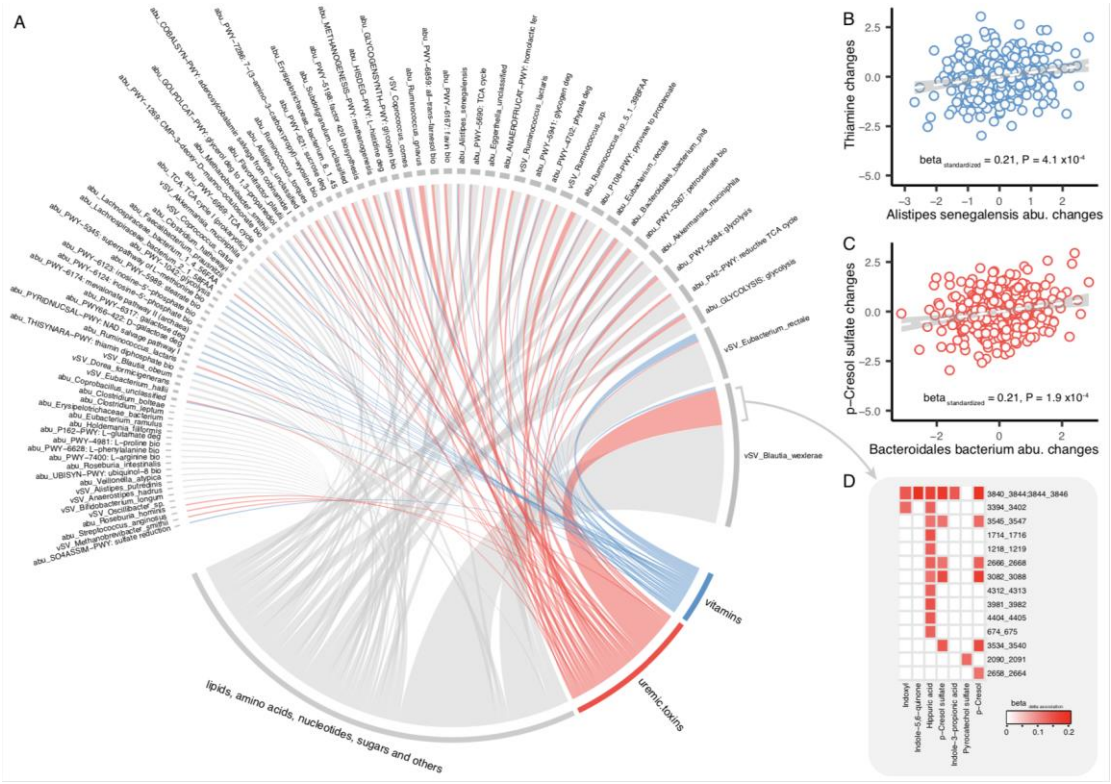

Figure 7. Casual mediation linkages among the gut microbiome, metabolites and phenotypes. A. 29 micorbial features associated with not only human phenotypes but also plasma metabolites. **B.** 21 significant mediation linkages. **C.** Microbial sulfate reduction pathway casually contributed to diastolic blood pressure through thiamine. **D.** Microbial lipopolysaccharides pathway casually contributed to systolic blood pressure

through AFMK. **E.** Ruminococcus sp vSV (300-305 kb) casually contributed to plasma LDL through tyrosol 4-sulfate.

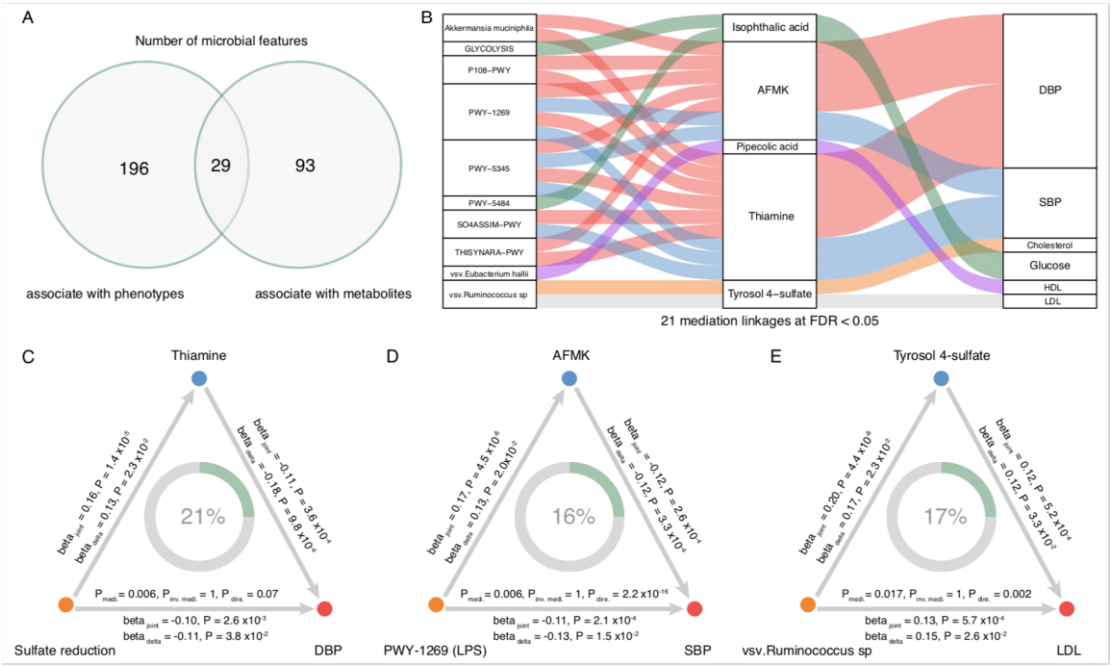

Figure 8. Long-term changes in antibiotic resistance genes and virulence factors. **A.** The total load of microbial antibiotic resistance genes increased between the two time points four years apart. **B.** The number of microbial virulence genes decreased over this time period. **C.** Positive associations between microbial species abundance changes and antibiotic resistance gene abundance changes. Red dots represent antibiotic resistance categories while blue dots indicate microbial species. **D.** Meat frequency positively associated with microbial aminoglycoside resistance gene abundance changes. **E.** Meat intake positively associated with microbial lincosamide resistance gene abundance changes.

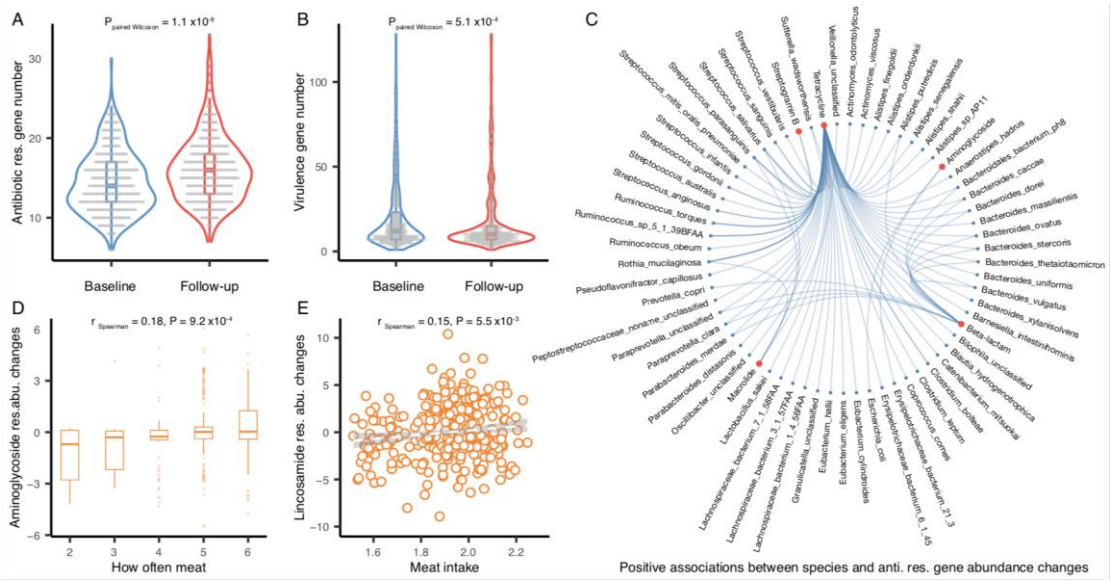
A
P paired Wilcoxon = 1.1 x10-9
Antibiotic res. gene number
Baseline
Follow-up
B
P paired Wilcoxon = 5.1 x10-4
Virulence gene number
Baseline
Follow-up
C
Positive associations between species and anti. res. gene abundance changes
D
r Spearman = 0.18, P = 9.2 x10-4
Aminoglycoside res.abu. changes
How often meat
E
r Spearman = 0.15, P = 5.5 x10-3
Lincosamide res. abu. changes
Meat intake

598

STAR ★ METHODS

KEY RESOURCES TABLE

REAGENT or RESOURCE	SOURCE	IDENTIFIER
Biological Samples		
Fecal samples	This study	
Blood samples	This study	
Critical Commercial Assays		
AllPrep DNA/RNA Mini Kit	QIAGEN	80204
Quant-iT PicoGreen dsDNA Assay	Life Technologies	P7589
Blood Assays	Lifelines Biobank	https://www.lifelines.nl
Software and Algorithms		
R (version 3.6.0)	R Foundation	http://www.r-project.org/
Python (version 2.7.11)	Python	https://www.python.org
KneadData (version 0.4.6.1)	The Huttenhower Lab	https://huttenhower.sph.harvard.edu/kneaddata
Bowtie2 (version 2.1.0)	(Langmead et al., 2019)	http://bowtie-bio.sourceforge.net/bowtie2
MetaPhlan2 (version 2.7.2)	(Truong et al., 2015)	https://huttenhower.sph.harvard.edu/metaphlan
HUMAnN2 (version 0.10.0)	(Franzosa et al., 2018)	https://huttenhower.sph.harvard.edu/humann
ShortBRED (version 0.9.5)	(Kaminski et al., 2015)	https://huttenhower.sph.harvard.edu/shortbred
StrainPhlAn (version 1.2.0)	(Truong et al., 2017)	http://segatalab.cibio.unitn.it/tools/strainphlan
ICRA	(Zeevi et al., 2019)	https://github.com/segalab/SGVFinder
SGVFinder	(Zeevi et al., 2019)	https://github.com/segalab/SGVFinder
Deposited Data		
LLD raw metagenomics	EGA	https://www.ebi.ac.uk
HMP raw metagenomics	HMP	https://www.hmpdacc.org

CONTACT FOR REAGENT AND RESOURCE SHARING

Further information and requests for resources and reagents should be directed to the Lead Contact, Jingyuan Fu (j.fu@umcg.nl).

EXPERIMENTAL MODEL AND SUBJECT DETAILS

Study cohort

The LifeLines-DEEP cohort is a sub-cohort of the LifeLines biobank (167,729 participants) (Scholtens et al., 2015) that involved 1,539 participants and is being used to assess the biomedical, socio-demographic, behavioral, physical, and psychological factors that contribute to health and disease from the north of the Netherlands (Tigchelaar et al., 2015; Wijmenga and Zhernakova, 2018). The study has been approved by Institutional ethics review board (IRB) of University Medical Center Groningen (ref. M12.113965). This cohort has now been followed-up, and detailed phenotypic data was collected at two time points around four years apart. Of the 1,135 individuals for whom we generated metagenomics sequencing data in 2013 (Zhernakova et al., 2016), follow-up stool samples were collected for 338 individuals (55.6% female and 44.4% male) at the second time point. The duration between two time points ranged from 3.33 to 3.92 years (mean=3.53, sd=0.12). At baseline, the mean age of participants was 48.2 years (18-80, sd=11.7) and their mean BMI was 25.4 (17.6-43.3, sd=4.08). For the follow-up, the mean age was 51.7 years (22-84, sd=11.7) and the mean BMI was 25.6 (16.1-37.6, sd=4.0). Phenotypic data assessed in the present study included 10 intrinsic factors (e.g. age, gender, BMI, height, smoking), 9 blood cell counts, 7 plasma metabolites (e.g. glucose, cholesterol, triglycerides) and 39 medications (e.g. PPI, oral contraceptives, beta blockers, statins).

METHOD DETAILS

Metagenomic data generation and preprocessing

Stool sample collection and processing at both time points followed the same protocol. All participants were asked to collect fecal samples at home and place them in their home freezer (-20°C) within 15 minutes after production. Subsequently, a nurse visited the participant to pick up the fecal samples on dry ice and transfer them to the laboratory. Aliquots were then made and stored at -80°C until further processing. The same protocol for fecal DNA isolation and metagenomics sequencing was used at both time points. Fecal DNA isolation was performed using the AllPrep DNA/RNA Mini Kit

(Qiagen; cat. 80204). After DNA extraction, fecal DNA was sent to the Broad Institute of Harvard and MIT in Cambridge, Massachusetts, USA, where library preparation and whole genome shotgun sequencing were performed on the Illumina HiSeq platform. From the raw metagenomic sequencing data, low-quality reads were discarded by the sequencing facility and reads belonging to the human genome were removed by mapping the data to the human reference genome (version NCBI37) with KneadData (version 0.4.6.1) Bowtie2 (version 2.1.0) (Langmead et al., 2019). The read depths of all samples at both time points were very comparable (paired Wilcoxon test P=0.89).

Taxonomic profiles

Microbial taxonomic profiles were generated using MetaPhlAn2 (version 2.7.2) (Truong et al., 2015). MetaPhlAn2 relies on nearly 1 million unique clade-specific marker genes identified from around 17,000 reference genomes (13,500 bacterial and archaeal, 3,500 viral and 110 eukaryotic), allowing unambiguous taxonomic assignments, accurate estimation of organismal relative abundance and species-level resolution for bacteria, archaea, eukaryotes and viruses. Microbial species present in more than 10% of the samples were included for further analyses. This yielded a list of 157 species that account for 97.81% of taxonomic composition.

Functional profiles

Microbial functional profiles were determined using HUMAnN2 (version 0.10.0) (Franzosa et al., 2018), which maps DNA/RNA reads to a customized database of functionally annotated pan-genomes. HUMAnN2 reported the abundances of gene families from the UniProt Reference Clusters (Bateman et al., 2015) (UniRef90), which were further mapped to microbial pathways from the MetaCyc metabolic pathway database (Caspi et al., 2016; Caspi et al., 2018). Based on MetaPhlAn2, HUMAnN2 can further characterize community functional profiles stratified by known (species-level) and unclassified organisms. In total, 343 microbial pathways present in more than 10% of the samples were kept for subsequent analysis, accounting for 99.98% of

660 microbial functional composition.

661 **Antibiotic resistance genes**

662 Quantification of antibiotic resistance genes in metagenomics was performed using
663 shortBRED (version 0.9.5) (Kaminski et al., 2015) with markers generated from the
664 ResFinder database, which reports more than 1,800 different antimicrobial resistance
665 genes (November 2018 version) (Zankari et al., 2012). In brief, ShortBRED is a
666 pipeline to take a set of protein sequences from a target database (i.e. ResFinder), cluster
667 them into families, build consensus sequences to represent the families, and then reduce
668 these consensus sequences to a set of unique identifying strings (markers). The pipeline
669 then searches for these markers in metagenomic data and determines the presence and
670 abundance of the protein families of interest. We classified the abundance of 29
671 antibiotic resistance genes that were present in at least 10% of the samples.

672 **Virulence genes**

673 We also searched the metagenomic data for bacterial virulence genes using shortBRED
674 (version 0.9.5) (Kaminski et al., 2015) and markers generated from virulence factors of
675 pathogenic bacteria database (VFDB, core dataset of DNA sequences, version:
676 November, 2018) (Liu et al., 2019). Here we classified the abundance of 59 virulence
677 genes that are present in at least 10% of the samples.

678 **Strain level SNP haplotypes**

679 Strain SNP haplotypes were generated using StrainPhlAn1 (version 1.2.0) (Truong et
680 al., 2017). This method is based on reconstructing consensus sequence variants within
681 species-specific marker genes and using them to estimate strain-level phylogenies.
682 Reconstructed markers with a percentage of ambiguous bases >20% are discarded.
683 Consensus sequences are then trimmed by removing the first and last 50 bases because
684 the terminal positions have lower coverages due to the limitations in mapping reads
685 against truncated sequences (Truong et al., 2017). Next, clades with a percentage of
686 markers <50% are removed, and if the percentage of samples in which a marker is

present is <50%, that marker is also removed. Samples with full sequences concatenated from all markers and a percentage of gaps >50% are removed from the alignment. Finally, we used the multiple sequence alignment file to generate a phylogenetic distance matrix that contains the pairwise nucleotide substitution rate between strains by applying the Kimura 2-parameter method from the EMBOSS package (Rice et al., 2000). Using this method, we classified the within-individual SNP haplotype difference of the dominant strain in 37 species that present in at least 5 sample pairs, and 18 of these were obtained in at least 10% of sample pairs.

Structural variants in microbial genome

We applied SGV-Finder pipeline (Zeevi et al., 2019) to classify SVs that are either completely absent in microbial genome of some samples (deletion SVs, dSVs) or those whose coverage is highly variable across samples (variable SVs, vSVs). Prior to SV classification, an 'iterative coverage-based read assignment' algorithm was applied that resolves ambiguous read assignments to regions that are similar between different bacteria, using information on bacterial relative abundances in the microbiome, their genomic sequencing coverage and sequencing and alignment qualities (Zeevi et al., 2019). In total, we classified 6,130 SVs, including 4,333 dSVs and 1,797 vSVs from 41 microbial species that present in at least 5 sample pairs. The SVs of 26 species can be obtained in at least 10% of sample pairs. We further calculated Canberra distance between individuals based on dSVs and vSVs of each microbial species, respectively.

Plasma untargeted metabolomics

Plasma samples of study participants were collected and frozen at -80°C with EDTA. During extraction, plasma samples were thawed on ice, vortexed, and spun down. 20μL of plasma was combined with 180μL of 80% methanol and vortexed for 15 seconds. The samples were incubated at 4°C for one hour to precipitate proteins, and then spun for 30 minutes at 3,200 RCF. 100μL of supernatant was removed and used for Flow-Injection Time-of-Flight Mass Spectrometry (FIA-TOF) analysis in General

714 Metabolics, Inc., Boston, USA, by using protocols described previously (Fuhrer et al.,
715 2011). In total, 1183 metabolites with annotations were involved in the analysis. The
716 annotated metabolites cover 18 chemical categories based on Human Metabolome
717 Database (HMDB) (**Table S2a**) (Wishart et al., 2018). The charactization of plasma
718 protein-bound uremic toxins, including indoxyl sulfate, p-cresyl sulfate, phenyl sulfate,
719 phenylacetic acid and hippuric acid was based on (Wang and Zhao, 2018).

720 **QUANTIFICATION AND STATISTICAL ANALYSIS**

721 **Principal coordinates analysis (PCoA)**

722 The relative abundances of all microbial species and pathways were included in PCoA.
723 We applied the *vegdist()* function from the *vegan* (version 2.5.5) R package to calculate
724 the Bray-Curtis dissimilarity matrix. Subsequently, classical metric multidimensional
725 scaling was carried out based on the Bray-Curtis distance matrix to obtain different
726 principal coordinates.

727 **Comparison of microbial composition dissimilarity**

728 To compare the differences in overall microbial species and pathway compositions
729 between- and within-individuals, we applied a Wilcoxon test on Bray-Curtis
730 dissimilarity. Since the number of dissimilarities between- and within-individuals was
731 unbalanced, we calculated an empiric P-value by permuting samples of microbial
732 species and pathway relative abundance tables for 10,000 times.

733 **Differential microbiome feature abundance**

734 We applied different transformation/normalization methods for the different microbial
735 abundance datasets, i.e. centered log-ratio transformation for relative abundances (sum
736 up to 1) of microbial species and functional pathways and log transformation (with
737 pseudo count of 1 for zero values) for microbial antibiotic resistance and virulence gene
738 abundance. Within-individual differences in microbial abundance were then assessed
739 by using paired Wilcoxon tests. The false discovery rate (FDR) was calculated with
740 1,000 times permutation.

Distance matrix-based individual classification

We evaluated if microbial abundance and genome information can be used for individual classification (i.e. to identify if two samples belong to the same individual). To do so, we generated Bray-Curtis distances based on microbial species and pathway relative abundance, Kimura distance based on SNP haplotype profile and Canberra distance based on SV profiles. The samples were clustered using single-linkage clustering, also known as nearest neighbor clustering. If two samples, and only those two samples, from the same individual were clustered together as the closest neighbor, we considered that they were classified correctly. We then defined the accuracy by calculating the proportion of the total number of correctly classified pairs. Finally, by establishing a specific cutoff, we could determine whether a pair of samples come from the same individual by their dissimilarity, and the cutoff affects the performance of classifier. A receiver operating characteristic curve (ROC) was drawn based on dissimilarity to reflect the specificity and sensitivity of classification using *roc()* function from *pROC* (version 1.16.1) (Robin et al., 2011).

Stepwise distance matrices combination

A total of 71 distance matrices were present in more than 10% of sample pairs, including 69 genetic distance matrices (SNP haplotype distance matrices for 18 species, dSV and vSV distance matrices for 26 species) and 2 compositional distance matrices generated by microbial species and pathways abundance. We aimed to see whether we can utilize these genetic and microbial distance matrices to classify different samples from the same individuals. Each of these distance matrices was considered as one classifier. We carried out a stepwise forward selection approach to combine multiple microbial genetic and compositional distance matrices. The cohort was randomly divided into a discovery set with 60% of sample pairs and a validation set with 40% of pairs. In order to combine multiple distance matrices, we first standardized and scaled all distance matrices between 0 and 1 by dividing each matrix by its largest value. In the discovery set, we assessed the accuracy of each distance matrix in classifying

samples as described above. We started with the distance matrix that had the highest accuracy, i.e. the 1st classifier. We then moved on to the model with two distance matrices by adding another distance matrix and taking the mean value of two matrices. We tested all possible combinations and chose the combination with the highest accuracy. The classifier included at the second step was considered as the 2nd classifier. This step was repeated to include the 3rd classifier, and this process continued until all the distance matrices were included. In this way, we generated a series of models that included different number of distance matrices and tested their performance in the validation set. The whole procedure of dataset splitting and feature combination was repeated 10 times, and we determined the optimal feature number *N* at which the performance did not improve anymore when more matrices were added. The distance-based features were prioritized by their median ranks across 10-times feature selections, then top-*N* distance matrices were selected as the optimum combination for the final classifier.

Microbial associations to host phenotypes and metabolites

We first established microbial associations to host phenotypes and metabolites (**Table S1**) using linear and logistic mixed-effects model (joint associations): dependent variable ~ (intercept) + independent variable + age + sex + (1| time point) + (1| subject), for continuous and binary microbial traits, respectively. We further validated these joint associations by linking microbial changes to host phenotypic and metabolic changes with a regression model (delta associations): dependent variable changes ~ (intercept) + independent variable changes + age + sex, for continuous and binary microbial traits (dSVs), respectively. The Benjamini-Hochberg procedure was applied to control FDR (Benjamini et al., 2001).

Casual mediation linkage inference

For phenotypic and metabolic associations to the same microbial fearure, we first checked whether human the phenotype associated with the metabolite by using both

796 joint and delat association models as described above. Next, bi-directional medication
797 analysis was carried out by using *mediate* function from mediation (version 4.5.0) R
798 package to inference casual role of microbiome in contributing to human phenotype
799 through metabolite. The Benjamini-Hochberg procedure was applied to control FDR.

800 **DATA AND SOFTWARE AVAILABILITY**

801 The raw metagenomic sequencing data of the Lifelines-DEEP and replication cohorts
802 are available from the European Genome-Phenome Archive (EGA,
803 https://www.ebi.ac.uk/ega/home) via accession number EGAS00001001704, and
804 Human Microbiome Project website (https://www.hmpdacc.org), respectively.
805 Analysis codes are available via: https://github.com/GRONINGEN-MICROBIOME-
806 CENTRE/Groningen-
807 Microbiome/tree/master/Projects/LLDeep_microbiome_5year_follow-up

REFERENCES

Aguilar-Barajas, E., Diaz-Perez, C., Ramirez-Diaz, M.I., Riveros-Rosas, H., and Cervantes, C. (2011). Bacterial transport of sulfate, molybdate, and related oxyanions. Biometals *24*, 687-707.

Alaei-Shahmiri, F., Soares, M.J., Zhao, Y., and Sherriff, J. (2015). The impact of thiamine supplementation on blood pressure, serum lipids and C-reactive protein in individuals with hyperglycemia: a randomised, double-blind cross-over trial. Diabetes Metab Syndr *9*, 213-217.

Aslam, B., Wang, W., Arshad, M.I., Khurshid, M., Muzammil, S., Rasool, M.H., Nisar, M.A., Alvi, R.F., Aslam, M.A., Qamar, M.U.*, et al.* (2018). Antibiotic resistance: a rundown of a global crisis. Infect Drug Resist *11*, 1645-1658.

Bateman, A., Martin, M.J., O'Donovan, C., Magrane, M., Apweiler, R., Alpi, E., Antunes, R., Ar-Ganiska, J., Bely, B., Bingley, M.*, et al.* (2015). UniProt: a hub for protein information. Nucleic Acids Res *43*, D204-D212.

Begley, T.P. (1996). The biosynthesis and degradation of thiamin (vitamin B1). Nat Prod Rep *13*, 177-185.

Benjamini, Y., Drai, D., Elmer, G., Kafkafi, N., and Golani, I. (2001). Controlling the false discovery rate in behavior genetics research. Behav Brain Res *125*, 279-284.

Caspi, R., Billington, R., Ferrer, L., Foerster, H., Fulcher, C.A., Keseler, I.M., Kothari, A., Krummenacker, M., Latendresse, M., Mueller, L.A.*, et al.* (2016). The MetaCyc database of metabolic pathways and enzymes and the BioCyc collection of pathway/genome databases. Nucleic Acids Res *44*, D471-D480.

Caspi, R., Billington, R., Fulcher, C.A., Keseler, I.M., Kothari, A., Krummenacker, M., Latendresse, M., Midford, P.E., Ong, Q., Ong, W.K.*, et al.* (2018). The MetaCyc database of metabolic pathways and enzymes. Nucleic Acids Res *46*, D633-D639.

Chen, L., Collij, V., Jaeger, M., van den Munckhof, I.C.L., Vich Vila, A., Kurilshikov, A., Gacesa, R., Sinha, T., Oosting, M., Joosten, L.A.B.*, et al.* (2020a). Gut microbial co-abundance networks show specificity in inflammatory bowel disease and obesity. Nature Communications *11*, 4018.

Chen, L., Garmaeva, S., Zhernakova, A., Fu, J., and Wijmenga, C. (2018). A system biology perspective on environment-host-microbe interactions. Hum Mol Genet *27*, R187-R194.

Chen, L., van den Munckhof, I.C.L., Schraa, K., Ter Horst, R., Koehorst, M., van Faassen, M., van der Ley, C., Doestzada, M., Zhernakova, D.V., Kurilshikov, A.*, et al.* (2020b). Genetic and Microbial Associations to Plasma and Fecal Bile Acids in Obesity Relate to Plasma Lipids and Liver Fat Content. Cell Rep *33*, 108212.

Coyte, K.Z., Schluter, J., and Foster, K.R. (2015). The ecology of the microbiome: Networks, competition, and stability. Science *350*, 663-666.

DiNicolantonio, J.J., Niazi, A.K., Lavie, C.J., O'Keefe, J.H., and Ventura, H.O. (2013). Thiamine supplementation for the treatment of heart failure: a review of the literature. Congest Heart Fail *19*, 214-222.

Duranton, F., Cohen, G., De Smet, R., Rodriguez, M., Jankowski, J., Vanholder, R., Argiles, A., and European Uremic Toxin Work, G. (2012). Normal and pathologic concentrations of uremic toxins. J Am Soc Nephrol *23*, 1258-1270.

Everard, A., Belzer, C., Geurts, L., Ouwerkerk, J.P., Druart, C., Bindels, L.B., Guiot, Y., Derrien,

M., Muccioli, G.G., Delzenne, N.M., *et al.* (2013). Cross-talk between Akkermansia muciniphila and intestinal epithelium controls diet-induced obesity. Proc Natl Acad Sci U S A *110*, 9066-9071.
Faith, J.J., Guruge, J.L., Charbonneau, M., Subramanian, S., Seedorf, H., Goodman, A.L., Clemente, J.C., Knight, R., Heath, A.C., Leibel, R.L., *et al.* (2013). The long-term stability of the human gut microbiota. Science *341*, 1-8.
Falony, G., Joossens, M., Vieira-Silva, S., Wang, J., Darzi, Y., Faust, K., Kurilshikov, A., Bonder, M.J., Valles-Colomer, M., Vandeputte, D., *et al.* (2016). Population-level analysis of gut microbiome variation. Science *352*, 560-564.
Franzosa, E.A., Huang, K., Meadow, J.F., Gevers, D., Lemon, K.P., Bohannan, B.J., and Huttenhower, C. (2015). Identifying personal microbiomes using metagenomic codes. Proc Natl Acad Sci U S A *112*, E2930-2938.
Franzosa, E.A., McIver, L.J., Rahnavard, G., Thompson, L.R., Schirmer, M., Weingart, G., Lipson, K.S., Knight, R., Caporaso, J.G., Segata, N., *et al.* (2018). Species-level functional profiling of metagenomes and metatranscriptomes. Nature Methods *15*, 962-968.
Fuhrer, T., Heer, D., Begemann, B., and Zamboni, N. (2011). High-Throughput, Accurate Mass Metabolome Profiling of Cellular Extracts by Flow Injection - Time-of-Flight Mass Spectrometry. Analytical Chemistry *83*, 7074-7080.
Garud, N.R., Good, B.H., Hallatschek, O., and Pollard, K.S. (2019). Evolutionary dynamics of bacteria in the gut microbiome within and across hosts. PLoS Biol *17*, e3000102.
Greenblum, S., Carr, R., and Borenstein, E. (2015). Extensive strain-level copy-number variation across human gut microbiome species. Cell *160*, 583-594.
Havelaar, A.H., Graveland, H., van de Kassteele, J., Zomer, T.P., Veldman, K., and Bouwknegt, M. (2017). A summary index for antimicrobial resistance in food animals in the Netherlands. BMC Vet Res *13*, 305.
Hornef, M.W., and Pabst, O. (2016). Real friends: Faecalibacterium prausnitzii supports mucosal immune homeostasis. Gut *65*, 365-367.
Joossens, M., Huys, G., Cnockaert, M., De Preter, V., Verbeke, K., Rutgeerts, P., Vandamme, P., and Vermeire, S. (2011). Dysbiosis of the faecal microbiota in patients with Crohn's disease and their unaffected relatives. Gut *60*, 631-637.
Kaminski, J., Gibson, M.K., Franzosa, E.A., Segata, N., Dantas, G., and Huttenhower, C. (2015). High-Specificity Targeted Functional Profiling in Microbial Communities with ShortBRED. PLoS Comput Biol *11*, e1004557.
Kikuchi, K., Saigusa, D., Kanemitsu, Y., Matsumoto, Y., Thanai, P., Suzuki, N., Mise, K., Yamaguchi, H., Nakamura, T., Asaji, K., *et al.* (2019). Gut microbiome-derived phenyl sulfate contributes to albuminuria in diabetic kidney disease. Nat Commun *10*, 1835.
Langmead, B., Wilks, C., Antonescu, V., and Charles, R. (2019). Scaling read aligners to hundreds of threads on general-purpose processors. Bioinformatics *35*, 421-432.
Liu, B., Zheng, D., Jin, Q., Chen, L., and Yang, J. (2019). VFDB 2019: a comparative pathogenomic platform with an interactive web interface. Nucleic Acids Res *47*, D687-D692.
Lloyd-Price, J., Arze, C., Ananthakrishnan, A.N., Schirmer, M., Avila-Pacheco, J., Poon, T.W., Andrews, E., Ajami, N.J., Bonham, K.S., Brislawn, C.J., *et al.* (2019). Multi-omics of the gut

892 microbial ecosystem in inflammatory bowel diseases. Nature *569*, 655-662.
893 Lloyd-Price, J., Mahurkar, A., Rahnavard, G., Crabtree, J., Orvis, J., Hall, A.B., Brady, A.,
894 Creasy, H.H., McCracken, C., Giglio, M.G., *et al.* (2017). Strains, functions and dynamics in
895 the expanded Human Microbiome Project. Nature *550*, 61-66.
896 Mayo, J.C., Sainz, R.M., Tan, D.X., Hardeland, R., Leon, J., Rodriguez, C., and Reiter, R.J.
897 (2005). Anti-inflammatory actions of melatonin and its metabolites, N1-acetyl-N2-formyl-5-
898 methoxykynuramine (AFMK) and N1-acetyl-5-methoxykynuramine (AMK), in macrophages.
899 J Neuroimmunol *165*, 139-149.
900 Mehta, R.S., Abu-Ali, G.S., Drew, D.A., Lloyd-Price, J., Subramanian, A., Lochhead, P., Joshi,
901 A.D., Ivey, K.L., Khalili, H., Brown, G.T., *et al.* (2018). Stability of the human faecal
902 microbiome in a cohort of adult men. Nat Microbiol *3*, 347-355.
903 Miquel, S., Martin, R., Rossi, O., Bermudez-Humaran, L.G., Chatel, J.M., Sokol, H., Thomas,
904 M., Wells, J.M., and Langella, P. (2013). Faecalibacterium prausnitzii and human intestinal
905 health. Curr Opin Microbiol *16*, 255-261.
906 Mishra, A.K., Gimenez, G., Lagier, J.C., Robert, C., Raoult, D., and Fournier, P.E. (2012).
907 Genome sequence and description of Alistipes senegalensis sp. nov. Stand Genomic Sci *6*, 1-
908 16.
909 Munukka, E., Rintala, A., Toivonen, R., Nylund, M., Yang, B., Takanen, A., Hanninen, A.,
910 Vuopio, J., Huovinen, P., Jalkanen, S., *et al.* (2017). Faecalibacterium prausnitzii treatment
911 improves hepatic health and reduces adipose tissue inflammation in high-fat fed mice. ISME J
912 *11*, 1667-1679.
913 Ochman, H., Lawrence, J.G., and Groisman, E.A. (2000). Lateral gene transfer and the nature
914 of bacterial innovation. Nature *405*, 299-304.
915 Ray, D., Alpini, G., and Glaser, S. (2014). Probiotic Bifidobacterium species: potential
916 beneficial effects in diarrheal disorders. Focus on "Probiotic Bifidobacterium species stimulate
917 human SLC26A3 gene function and expression in intestinal epithelial cells". Am J Physiol Cell
918 Physiol *307*, C1081-1083.
919 Rezzani, R., Porteri, E., De Ciuceis, C., Bonomini, F., Rodella, L.F., Paiardi, S., Boari, G.E.,
920 Platto, C., Pilu, A., Avanzi, D., *et al.* (2010). Effects of melatonin and Pycnogenol on small
921 artery structure and function in spontaneously hypertensive rats. Hypertension *55*, 1373-1380.
922 Rice, P., Longden, I., and Bleasby, A. (2000). EMBOSS: the European Molecular Biology Open
923 Software Suite. Trends Genet *16*, 276-277.
924 Robin, X., Turck, N., Hainard, A., Tiberti, N., Lisacek, F., Sanchez, J.C., and Muller, M. (2011).
925 pROC: an open-source package for R and S+ to analyze and compare ROC curves. BMC
926 Bioinformatics *12*, 77.
927 Rothschild, D., Weissbrod, O., Barkan, E., Kurilshikov, A., Korem, T., Zeevi, D., Costea, P.I.,
928 Godneva, A., Kalka, I.N., Bar, N., *et al.* (2018). Environment dominates over host genetics in
929 shaping human gut microbiota. Nature *555*, 210-215.
930 Schloissnig, S., Arumugam, M., Sunagawa, S., Mitreva, M., Tap, J., Zhu, A., Waller, A., Mende,
931 D.R., Kultima, J.R., Martin, J., *et al.* (2013). Genomic variation landscape of the human gut
932 microbiome. Nature *493*, 45-50.
933 Scholtens, S., Smidt, N., Swertz, M.A., Bakker, S.J., Dotinga, A., Vonk, J.M., van Dijk, F., van

Zon, S.K., Wijmenga, C., Wolffenbuttel, B.H., *et al.* (2015). Cohort Profile: LifeLines, a three-generation cohort study and biobank. Int J Epidemiol *44*, 1172-1180.
Silva, S.O., Rodrigues, M.R., Carvalho, S.R., Catalani, L.H., Campa, A., and Ximenes, V.F. (2004). Oxidation of melatonin and its catabolites, N1-acetyl-N2 -formyl-5-methoxykynuramine and N1-acetyl-5-methoxykynuramine, by activated leukocytes. J Pineal Res *37*, 171-175.
Solomon, S.D., Uno, H., Lewis, E.F., Eckardt, K.U., Lin, J., Burdmann, E.A., de Zeeuw, D., Ivanovich, P., Levey, A.S., Parfrey, P., *et al.* (2010). Erythropoietic response and outcomes in kidney disease and type 2 diabetes. N Engl J Med *363*, 1146-1155.
Stewart, C.J., Ajami, N.J., O'Brien, J.L., Hutchinson, D.S., Smith, D.P., Wong, M.C., Ross, M.C., Lloyd, R.E., Doddapaneni, H., Metcalf, G.A., *et al.* (2018). Temporal development of the gut microbiome in early childhood from the TEDDY study. Nature *562*, 583-588.
Tigchelaar, E.F., Zhernakova, A., Dekens, J.A., Hermes, G., Baranska, A., Mujagic, Z., Swertz, M.A., Munoz, A.M., Deelen, P., Cenit, M.C., *et al.* (2015). Cohort profile: LifeLines DEEP, a prospective, general population cohort study in the northern Netherlands: study design and baseline characteristics. BMJ Open *5*, e006772.
Truong, D.T., Franzosa, E.A., Tickle, T.L., Scholz, M., Weingart, G., Pasolli, E., Tett, A., Huttenhower, C., and Segata, N. (2015). MetaPhlAn2 for enhanced metagenomic taxonomic profiling. Nat Methods *12*, 902-903.
Truong, D.T., Tett, A., Pasolli, E., Huttenhower, C., and Segata, N. (2017). Microbial strain-level population structure and genetic diversity from metagenomes. Genome Res *27*, 626-638.
Vacca, I. (2017). Biofilms: New ways for streptococci to settle down. Nat Rev Microbiol *15*, 321.
Vatanen, T., Franzosa, E.A., Schwager, R., Tripathi, S., Arthur, T.D., Vehik, K., Lernmark, A., Hagopian, W.A., Rewers, M.J., She, J.X., *et al.* (2018). The human gut microbiome in early-onset type 1 diabetes from the TEDDY study. Nature *562*, 589-594.
Vatanen, T., Plichta, D.R., Somani, J., Munch, P.C., Arthur, T.D., Hall, A.B., Rudolf, S., Oakeley, E.J., Ke, X., Young, R.A., *et al.* (2019). Genomic variation and strain-specific functional adaptation in the human gut microbiome during early life. Nat Microbiol *4*, 470-479.
Veloo, A.C.M., Baas, W.H., Haan, F.J., Coco, J., and Rossen, J.W. (2019). Prevalence of antimicrobial resistance genes in Bacteroides spp. and Prevotella spp. Dutch clinical isolates. Clin Microbiol Infect *25*, 9-13.
Vich Vila, A., Imhann, F., Collij, V., Jankipersadsing, S.A., Gurry, T., Mujagic, Z., Kurilshikov, A., Bonder, M.J., Jiang, X., Tigchelaar, E.F., *et al.* (2018). Gut microbiota composition and functional changes in inflammatory bowel disease and irritable bowel syndrome. Sci Transl Med *10*, eaap8914.
Vieira-Silva, S., Falony, G., Belda, E., Nielsen, T., Aron-Wisnewsky, J., Chakaroun, R., Forslund, S.K., Assmann, K., Valles-Colomer, M., Nguyen, T.T.D., *et al.* (2020). Statin therapy is associated with lower prevalence of gut microbiota dysbiosis. Nature *581*, 310-315.
Wang, Z., and Zhao, Y. (2018). Gut microbiota derived metabolites in cardiovascular health and disease. Protein Cell *9*, 416-431.
Wijmenga, C., and Zhernakova, A. (2018). The importance of cohort studies in the post-GWAS

era. Nat Genet, 322-328.
Wishart, D.S., Feunang, Y.D., Marcu, A., Guo, A.C., Liang, K., Vazquez-Fresno, R., Sajed, T., Johnson, D., Li, C., Karu, N., *et al.* (2018). HMDB 4.0: the human metabolome database for 2018. Nucleic Acids Res *46*, D608-D617.
Yassour, M., Jason, E., Hogstrom, L.J., Arthur, T.D., Tripathi, S., Siljander, H., Selvenius, J., Oikarinen, S., Hyoty, H., Virtanen, S.M., *et al.* (2018). Strain-Level Analysis of Mother-to-Child Bacterial Transmission during the First Few Months of Life. Cell Host Microbe *24*, 146-154.
Yu, T.-H., Tang, W.-H., Lu, Y.-C., Wang, C.-P., Hung, W.-C., Wu, C.-C., Tsai, I.-T., Chung, F.-M., Houng, J.-Y., and Lan, W.-C. (2018). Association between hippuric acid and left ventricular hypertrophy in maintenance hemodialysis patients. Clinica Chimica Acta *484*, 47-51.
Zankari, E., Hasman, H., Cosentino, S., Vestergaard, M., Rasmussen, S., Lund, O., Aarestrup, F.M., and Larsen, M.V. (2012). Identification of acquired antimicrobial resistance genes. J Antimicrob Chemother *67*, 2640-2644.
Zeevi, D., Korem, T., Godneva, A., Bar, N., Kurilshikov, A., Lotan-Pompan, M., Weinberger, A., Fu, J., Wijmenga, C., Zhernakova, A., *et al.* (2019). Structural variation in the gut microbiome associates with host health. Nature *568*, 43-48.
Zhao, H., Shen, J., Djukovic, D., Daniel-MacDougall, C., Gu, H., Wu, X., and Chow, W.H. (2016). Metabolomics-identified metabolites associated with body mass index and prospective weight gain among Mexican American women. Obes Sci Pract *2*, 309-317.
Zhernakova, A., Kurilshikov, A., Bonder, M.J., Tigchelaar, E.F., Schirmer, M., Vatanen, T., Mujagic, Z., Vila, A.V., Falony, G., Vieira-Silva, S., *et al.* (2016). Population-based metagenomics analysis reveals markers for gut microbiome composition and diversity. Science *352*, 565-569.
Zhou, W., Sailani, M.R., Contrepois, K., Zhou, Y., Ahadi, S., Leopold, S.R., Zhang, M.J., Rao, V., Avina, M., Mishra, T., *et al.* (2019). Longitudinal multi-omics of host-microbe dynamics in prediabetes. Nature *569*, 663-671.